Available online at www.sciencedirect.com
ScienceDirect
C. R. Physique 8 (2007) 865–883
COMPTES RENDUS PHYSIQUE
http://france.elsevier.com/direct/COMREN/

Neutron scattering/Diffusion de neutrons

# Structural and dynamical studies from bio-mimetic systems: an overview

Giovanna Fragneto [a,*], Maikel Rheinstädter [b]

[a] *Institut Laue-Langevin, 6, rue Jules Horowitz, B.P. 156, 38042 Grenoble cedex 9, France*
[b] *Department of Physics and Astronomy, 223 Physics Building, University of Missouri-Columbia, Columbia, MO 65211, USA*

Available online 30 October 2007

**Abstract**

Membranes are ubiquitous in living materials and carry out highly specialised functions. They surround both cells (plasma membranes) and organelles within cells and represent the surface through which interaction occurs with the outside world. Cell membranes consist mostly of lipids and proteins. Scientists have been well aware for a long time of the importance of lipid structural properties for understanding functional mechanisms at membrane surfaces. Neutron scattering techniques are powerful tools for the characterization of the structure and dynamics of bio-mimetic systems and much progress has been done in recent years since they give the unique access to microscopic structure and dynamics at length scales of intermolecular or atomic distances. The optimization of instrumentation and sample preparation techniques, as well as the new possibilities offered by protein deuteration, have opened the way to studies of lipid/protein interactions that were impossible in the past. It is now possible to engineer systems that allow one to look at the insertion of biomolecules into membranes and to determine very accurately the structure as well as the dynamics of the interaction. ***To cite this article: G. Fragneto, M. Rheinstädter, C. R. Physique 8 (2007).***


**Résumé**

**Études structurales et dynamiques de systèmes bio-mimétiques.** Les membranes existent partout dans les matériaux vivants et portent des fonctions hautement spécialisées. Elles entourent à la fois les cellules (membranes cellulaires) et les organites intra-cellulaires. Elles correspondent à la surface à travers laquelle se fait l'interaction avec le monde extérieur. Les membranes des cellules consistent essentiellement de lipides en protéines. Les scientifiques ont réalisé depuis longtemps l'importance des propriétés structurales des lipides pour la compréhension des mécanismes fonctionnels à la surface de la membrane. Les techniques de diffusion de neutrons sont un outil puissant pour caractériser à la fois la structure et la dynamique des systèmes bio-mimétiques. Ces dernières années, beaucoup de progrès ont été réalisés grâce à cet accès unique à la structure microscopique ainsi qu'à la dynamique sur des échelles de longueurs interatomiques et intermoléculaires. L'optimisation de l'instrumentation et les techniques de préparation de l'échantillon ainsi que les nouvelles possibilités offertes par la deutériation des protéines ont ouvert la voie aux études des interactions lipides/protéines, interdites jusqu'ici. Il est maintenant possible de créer des systèmes qui permettent de regarder l'insertion des biomolécules dans les membranes et de déterminer précisément leur structure et la dynamique associée aux interactions. ***Pour citer cet article : G. Fragneto, M. Rheinstädter, C. R. Physique 8 (2007).***


*Keywords:* Bio-mimetic systems; Neutron scattering

* Corresponding author.
*E-mail address:* fragneto@ill.fr (G. Fragneto).

1631-0705/$ – see front matter 
doi:10.1016/j.crhy.2007.09.003

*Mots-clés :* Système bio-mimétique ; Diffusion de neutrons

## 1. Introduction: why model membrane studies are interesting

The understanding of the complexity of living cells is one of the challenges of physics in our century. Living cells provide an inspiration for research in soft matter physics and represent also the ultimate goal in nanotechnology. They are made up of molecular assemblies, which are 'self-organized'; they have many different length scales, from the atomic (nm) to the microscopic (μm) and their dynamics exhibit many different time scales from picoseconds to hours. The way physics works is to try to 'model' these behaviors with simple systems and many examples can be found in modern materials science.

Cell membranes consist mostly of lipids and proteins although sterols are other important constituents that, for example, can make up to 20 wt% of the lipid composition of plasma membranes. The entire membrane is held together by the non-covalent interaction of hydrophobic tails: phospholipid molecules are nevertheless free to diffuse laterally even though movement between layers is not energetically favourable.

The cell wall plays mostly a mechanical support role: one of its key roles is to maintain the cell potential. The functions of the cell membrane include: (i) sorting what enters and exits the cell; (ii) molecule transportation by way of ion pumps and channels and carrier proteins; (iii) hosting receptors that allow chemical messages to be exchanged between cells and systems; (iv) anchoring of the cytoskeleton to provide the shape to the cell; (v) participation in enzyme activity important, for example, in metabolism or immunity.

The determination of the structure of cell membranes alone or while interacting with proteins, enzymes, DNA, etc., is a fundamental pre-requisite to understand function. Beside the interest in fundamental science, both in the fields of cell biology and more generally in soft matter physics, the study of cell membranes is boosted by applications in nanotechnology and bio-inspired materials science. For example, transmembrane proteins and membrane-associated proteins are targeted in many infectious diseases. Membrane models are extremely important for understanding the fundamental cellular processes involved and in screening for pathogens or drug candidates. Supported membranes can be patterned and manipulated in many ways to tune their architecture and physical properties for optimal immobilization of membrane proteins. This is expected to be vastly exploited for biosensors and detection of protein functions at the molecular level.

The lateral structure of membranes including both height and compositional fluctuations remains an important experimental challenge of present-day biophysics, concerning in particular the biologically relevant fluid L$\alpha$ state, where the material softness compromises the use of scanning probe microscopy. In 'real' space, probes like atomic force and electron microscopies can only provide *localized* images of structures on surfaces. On the other hand, scattering techniques employing neutrons or X-rays have proven invaluable for looking at large areas and can contribute to the elucidation of the molecular structure as well as to the understanding of molecular and supramolecular dynamics of lipid bilayers.

## 2. How are cell membranes modeled

Because of the complexity of cell membranes (cf. cartoon in Fig. 1), good and biologically relevant models of cell membranes are not easy to produce [1]. It has been common practice in recent years to try to gain understanding in the behavior of cell membranes starting from the structural characterization of their basic components, with the lipid bilayer being considered as the simplest model of all [2].

Lipids are amphiphilic molecules consisting of a hydrophilic head and hydrophobic double chains (saturated and un-saturated) (cf. Fig. 2). They form a continuous bilayer, which acts as a barrier to water soluble molecules and provides the framework for the incorporation of membrane proteins. The physico-chemical properties of lipids in membranes are subject to important requirements; the acyl chains must be in a liquid state to keep the membrane proteins active and lipids must form a bilayer structure so that the membrane acts as an insulating barrier. However, the ability of lipids to form also non-bilayer structures seems to be a pre-requisite for several membrane associated processes [3].

Scientists have been well aware for a long time of the importance of lipid structural properties for understanding functional mechanisms at membrane surfaces and studies on lipid bilayers have proliferated in the 1970s and 1980s.

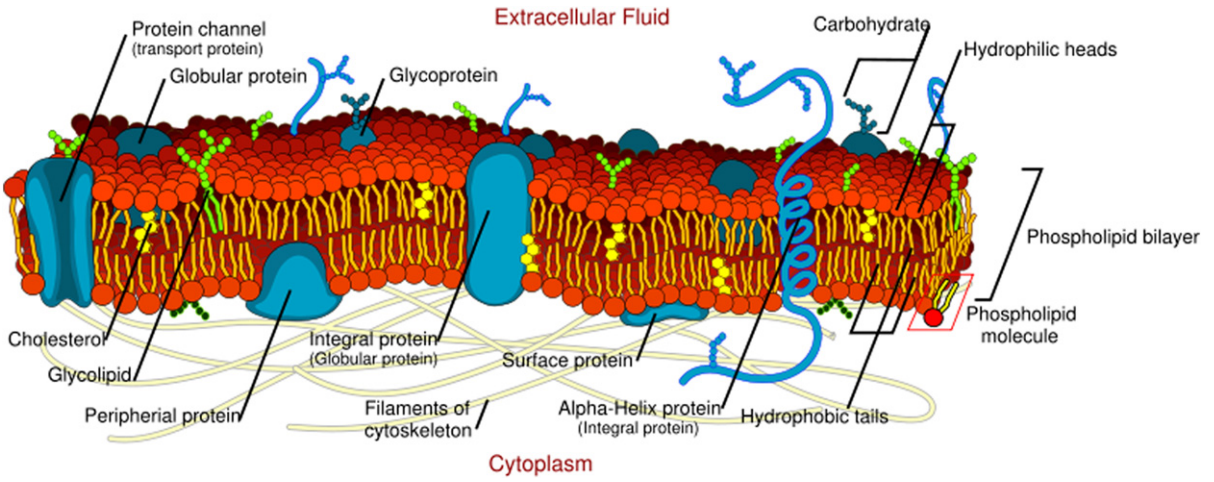


Fig. 1. Sketch of a cell membrane.

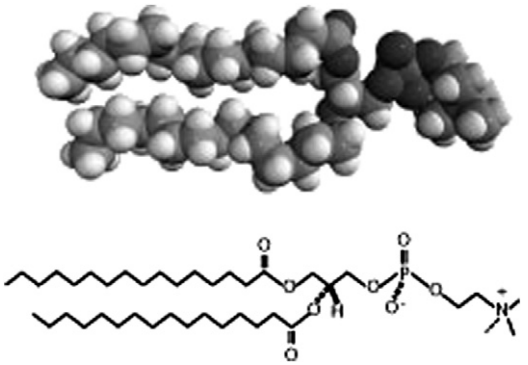

Fig. 2. Chemical composition and space filling model of a common phospholipid used in model membrane studies: 1,2-dipalmitoyl-sn-glycero-3-phosphocholine (DPPC).

In the last few years we have witnessed the revival of this classical approach for mimicking cell membranes. This is due mainly to the availability of a certain number (although still low) of membrane protein structures, that have elucidated some of the mechanisms happening at cell surfaces, and to the advent of new or improvement of existing structural techniques enabling studies of single bilayers with a fraction of a nanometer resolution.

Although bilayers in membranes contain variable amounts of cholesterol, the simplest models make use only of phospholipids. Saturated chains, and the use of a single type of molecules, help preparing ordered samples; on the opposite, unsaturated chains, or mixtures of different molecules, favor bilayer fluidity. As for lipid heads, phosphatidyl-cholines (or PC, or phosphocholines) are widely used. Charged heads (e.g. phosphatidyl-serine, PS), often mixed with variable ratios of neutral heads, help controlling the bilayer charge. A variety of sample types have been tried. Some examples are shown schematically in Fig. 3 and described now.

### 2.1. *Lipid monolayers*

Lipid monolayers at the air-water interface (Fig. 3(a)) are commonly referred to as *Langmuir monolayers* and they are prepared by spreading a solution of lipids on the surface of water in a Langmuir trough [4]. A pressure captor can monitor the surface pressure and a compression barrier can control the lipid density. With a slightly more sophisticated apparatus, monolayers can be prepared also at the oil–water interface.

An interesting feature of spread monolayers on water is their versatility: lipid composition may be tailored at will, provided that insoluble molecules are used. The direct access through air, and the good planarity of the layer, facilitates many studies such as X-ray and neutron reflectivity, and other surface techniques such as surface-sensitive infrared

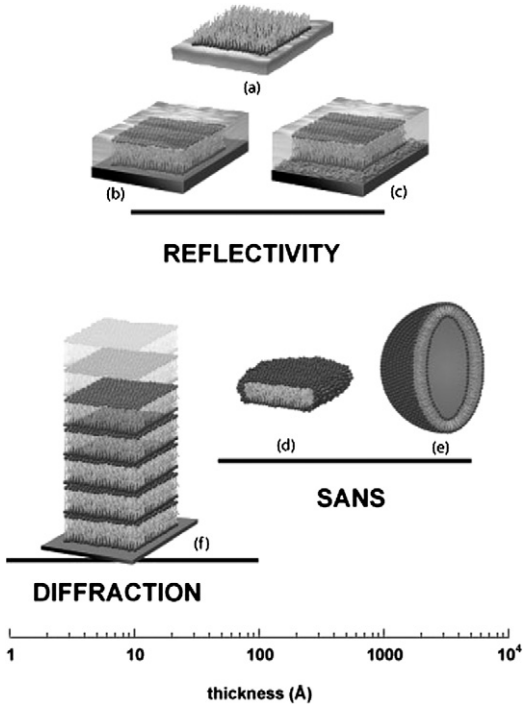


Fig. 3. Distances and $q$-ranges probed by the techniques discussed in the text. Schematic drawings of: (a) a monolayer at the air–water interface; (b) a bilayer deposited on a solid substrate; (c) a floating bilayer; (d) a bilayered micelle (bicelle); (e) a small unilamellar vesicle (SUV); (f) stacked bilayers.

spectroscopy or Brewster Angle microscopy. Their interest stems from the fact that many physiologically important interactions take place at the interface between the membrane, for example at the lipid head groups, and the aqueous compartment.

### 2.2. *Lipid single bilayers*

Supported lipid bilayers (Fig. 3(b)) can be deposited on solid substrates in various ways. They allow bio-functionalisation of inorganic solids (semiconductors, gold covered surfaces, opto-electronic devices) and polymeric materials, as well as imaging by atomic force microscopy [5].

Protocols for the deposition by vesicle fusion go back to McConnell et al. [6]. Well-defined structures can be obtained with modified Langmuir troughs and the so-called Langmuir–Blodgett or Langmuir–Schaeffer techniques [7]. These are well-defined structures, where the composition of each leaflet of the bilayer can be chosen separately. The proximity of the substrate limits the position fluctuation, which is a disadvantage when studying the interaction with transmembrane proteins.

Other approaches for the formation of planar single lipid bilayers less interacting with the solid substrate are being tried. One is vesicle spreading on polymer layers, where the polymer provides a soft cushion screening the influence of the substrate. An interesting review on polymer-supported membranes (Fig. 3(c)) as models of the cell surface is to be found in [8].

Recently, Charitat et al. [9] have succeeded in the preparation of stable and reproducible double bilayers, in which a lipid bilayer floats at 20–30 Å on top of one adsorbed on a solid substrate. This system has made it possible to perform reflectivity studies on a highly hydrated, accessible and fluctuating bilayer, where the composition of each leaflet can be chosen separately. It has proved to be very useful to probe bilayer–bilayer interactions [10,11], and showed to be stable after inclusion of cholesterol [12,13] as well as of charges in water and in the bilayer [14], so that interactions with other molecules relevant for biology studies can be determined in physiological buffer.

### 2.3. Multilamellar stacks and vesicles

Vesicles, or liposomes, are bilayers closed in roughly spherical shapes, which enclose a fixed volume of water or solution. They allow one to control the composition not only of the lipid bilayers, but also of both the outer and inner medium. The environment can be tailored (pH, ionic strength, etc.) to match those found under physiological conditions. It is, e.g., possible to prepare the vesicles in a solution with high osmotic pressure, and rinse them in a solution with a slightly smaller pressure, so that the water flows inwards: the vesicles then swell and become under tension. This dramatically reduces the position fluctuations of the membrane, which amplitude is thus under the experimentalist control.

These vesicles are usually small, typically tens or hundreds of nanometers, and are multilamellar. Forcing the vesicles to flow through a filter with a controlled pore size (an 'extruder') results in a population of small (mostly) unilamellar vesicles, or SUV (Fig. 3(e)).

Over the past decade 'bicellar' lipid mixtures composed of the long-chain dimyristoyl phosphatidylcholine (DMPC) and the short-chain dihexanoyl PC (DHPC) molecules have emerged as a powerful medium for studying membrane associated, biologically relevant macromolecules and assemblies (Fig. 3(d)). Depending on temperature, lipid concentration and composition these lipid mixtures can assume a variety of morphologies, some of them alignable in the presence of a magnetic field.

Multilamellar stacks of bilayers have been prepared and used for a long time (Fig. 3(f)) [15]. They are suitable for diffraction as well as inelastic scattering (see below), due to the large amount of material involved. The most common way of aligning lipid multibilayers is to deposit them from a concentrated lipid/solvent solution onto the solid support (typically glass or silicon) and allow the solvent to slowly evaporate in order to get highly aligned samples. Then, they are hydrated in water-saturated atmosphere. The current efforts have been particularly successful in two directions: (i) in increasing the hydration, going up to full hydration (100% of the vapour pressure) [16]; (ii) in improving the control of both the number of stacked bilayers (from a few units to a few hundreds) and their order (parallelism of bilayers of order of a fraction of degree), making possible to perform simultaneously diffraction and reflectivity on the same sample [17].

## 3. What can neutrons reveal?

The wavelength of neutron and X-ray beams is of the order of the tenth of a nanometer; therefore they are ideal tools for the structural and dynamical characterisation of lipid bilayers (the thickness of cell membranes is $\sim$5 nm). The specific properties of the neutrons make them ideal probes for investigations in soft-matter and biology. Biological membrane components, like most soft materials, are rich in hydrogen, and neutrons have the unique capability of being scattered differently from hydrogen and deuterium. It is thus possible to choose the $H_2O/D_2O$ water composition so that the water matrix has the same cross section as parts of the sample with the effect that there will be no signal from those regions. This technique is known as *contrast variation*. It is also possible to accentuate or annihilate the scattering from individual parts of a macromolecular complex so, for example, by specific deuterium labeling it is possible to measure bilayer conformational changes and organization both in the perpendicular and lateral directions [18,19]. Fig. 4 shows the differential scatter of various types of biological macromolecules as a function of the $D_2O$ concentration. Table 1 shows the scattering lengths for various elements (in $10^{-12}$ cm).

Since neutrons interact weakly with atomic nuclei, they are highly penetrating so that samples in complex sample environments can be probed and in-situ measurements from buried interfaces are possible. Finally, neutron energies range from the meV to the eV and therefore they are comparable to the energies of atomic and electronic processes. This allows for the study of dynamic properties like translations, vibrations, rotations, lattice modes, exhibited by molecules.

Near-field microscopies have enjoyed over two decades of successful developments. However, they have not replaced experiments using X-rays or neutrons (the so-called 'Fourier space' techniques). Direct measurements ('real space' techniques) include atomic force microscopy, near-field scanning optical microscopy, surface force apparatus, second-harmonic generation, micromanipulation, and interference microscopy. The past decade proved how useful are the complementary information obtained in real space and Fourier space: more and more publications actually include simultaneously one technique of each type [20].

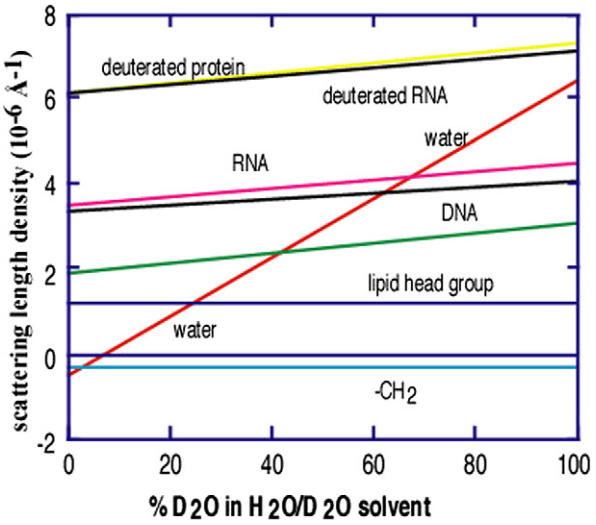


Fig. 4. Illustration of contrast matching, i.e. the differential scatter of various types of biological macromolecules as a function of the $D_2O$ concentration.

Table 1
Scattering lengths for different elements ($10^{-12}$ cm)

| H | D | C | N | O | P | S |
|---|---|---|---|---|---|---|
| −0.3742 | 0.6671 | 0.6651 | 0.940 | 0.5804 | 0.517 | 0.2847 |

## 4. Results from structural studies: elastic methods

Lipid membranes are disordered systems. It is not possible to use crystallography measurements for a high-resolution structural characterization. The elastic neutron scattering techniques which have been mostly employed in the past for membrane studies, are: (i) *Small angle scattering* (SAS), used to gain information on shape, size and interactions of lipid lamellar systems and vesicles: it gives radial averaged information in all directions of space; (ii) *Small and Wide Angle Diffraction*, used mainly to determine the in-plane and normal structure of stacked lipid lamellar systems; (iii) *Specular reflectivity*, used to study the structure of bilayers in the direction perpendicular to the plane of the layers in a planar configuration. In all cases experimental set-ups consist of: a radiation source, a wavelength selector or choppers, a system of collimation, the sample and a system of detection.

The principle of these types of experiments is represented in Fig. 5. A collimated incoming beam of wavelength $\lambda$ interacts with a sample with an angle of incidence. The outgoing beam at an angle $\theta$ from the sample is measured by a detector (punctual, mono or bi-dimensional). The angle between the incoming and outgoing beams is defined as the scattering angle, $2\theta$. The intensity of the outgoing over that of the incoming beams is recorded vs. the wave vector transfer, $q$. This is the modulus of the resultant between the incident, $k_i$, and scattered, $k_r$, wavevectors, and is given by:

$$q = \frac{4\pi}{\lambda} \sin\theta \tag{1}$$

Different types of experiments can be performed: (i) in reflection or in transmission; (ii) with an angular range going from a few mdeg to 100 degrees ($q$ value from $10^{-3}$ to 1 $\text{Å}^{-1}$); (iii) with a beam of one defined wavelength, by scanning the angle of incidence and the angle of emergence (so called *monochromatic mode*); (iv) at a fixed angle of incidence, using a polychromatic incident beam (so called *time-of-flight mode*). Note that only the amplitudes of the scattered waves can be measured, while the phase shifts cannot be determined directly. This is the well-known 'phase problem' which usually inhibits a direct transformation back into real space.

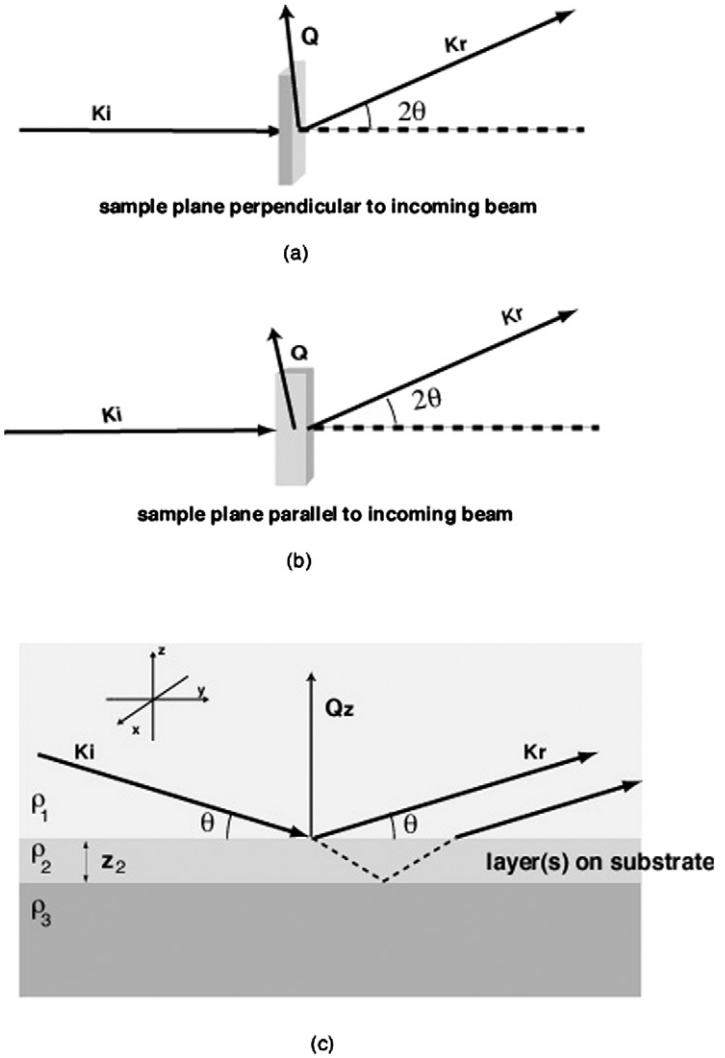


Fig. 5. Schematic layout of a scattering experiment in (a) transmission or (b) reflection and (c) a specular reflectivity experiment.

### *4.1. Small angle scattering*

Small angle scattering experiments provide information about the size, shape and orientation of the different components of a sample for distances ranging from 50 to 5000 Å.

Experiments are generally performed in transmission conditions (with the sample fixed) and measuring the intensity for very low $2\theta$ angles (with a 2-dimensional detector). Measurements are generally performed in situ and following changes from external conditions.

The objective of a SANS experiment is to determine the differential cross-section since it contains all the information on the shape, size and interactions of the scattering bodies in the sample. The differential cross-section for monodisperse spheres is given by the approximate relation:

$$\frac{\mathrm{d}\sigma}{\mathrm{d}\Omega}(q) = N_p V_p^2 (\Delta\rho)^2 P(q) S(q) + B_{\mathrm{inc}} \tag{2}$$

where $N_p$ is the number concentration of scattering bodies (given the subscript '$p$' for 'particles'), $V_p$ is the volume of one scattering body, $P(q)$ is a function known as the form or shape factor, $S(q)$ is the interparticle structure factor and $B_{\mathrm{inc}}$ is the (isotropic) incoherent background signal. $(\Delta\rho)^2$ is the square of the difference in neutron scattering length

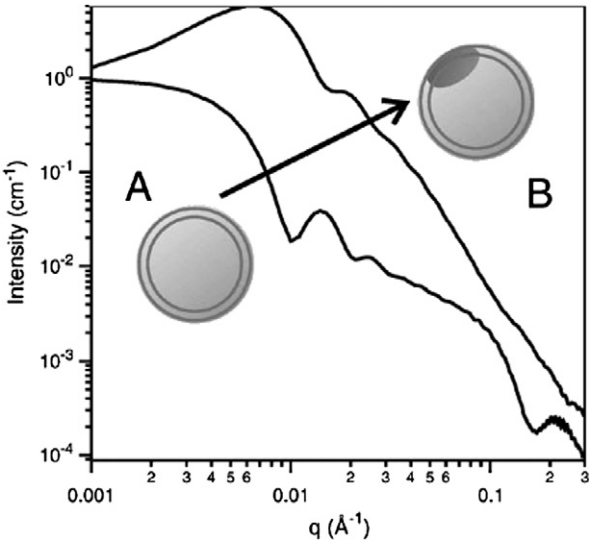


Fig. 6. SANS from unilamellar vesicles; schematic representation of lateral segregation adapted from [22].

density, $\rho = \sum_i n_i b_i$ where $n_i$ and $b_i$ are respectively the number of atoms and scattering length of the species $i$. $(\mathrm{d}\sigma/\mathrm{d}\Omega)(q)$ has dimensions of (length)$^{-1}$ and is normally expressed in units of cm$^{-1}$.

For non-interacting objects with a radius of gyration $R_G$ and $q \ll 1/R_G$, the plot of $\ln I(q)$ versus $q^2$ results in a straight line of slope $-R_G^2/3$ commonly referred to as Guinier plot. When $q$ is large enough, $I(q)$ decays as $q^{-\alpha}$, where $\alpha$ is related to the fractal dimension or roughness of the surface.

While for polymeric materials SANS is the single most important neutron scattering technique, used for probing size, shape and conformation of macromolecular complexes, in the case of biologically relevant materials, the technique is employed to study systems under physiologically meaningful conditions as well as disordered materials that are difficult or impossible to crystallize. SANS can be used to characterise the stability of biological membranes interacting with additive molecules. Pharmacologically important molecules that in appropriate concentrations help the stabilization of lipid bilayers or the undergoing of structural transitions can be investigated [21]. For a recent review on the study of membranes using small angle neutron scattering see [22].

Fig. 6 shows an example adapted from [18,22] where recent SANS measurements are reported on the lateral segregation in unilamellar vesicles by use of contrast variation methods. The interest in membrane domains is driven by their potential role in a variety of biological functions like immune response, synaptic transmission, intracellular trafficking or as platforms for infection by viruses such as HIV. Despite the number of studies carried out over the years, there is still a controversy regarding domain sizes and lifetimes. The most fashionable models describe rafts (functional domains) as transient clusters undergoing continual formation and dispersion that can coalesce and stabilize larger functional domains in response to particular signals. It is widely accepted that cholesterol is one of the key components of lipid rafts. It is more and more commonly accepted that lipid rafts in vivo are spatio-temporally regulated by the cell rather than being passively formed by thermally equilibrated systems; nevertheless studies on model systems provide valuable information as to the relative importance of lipids and cholesterol in stabilizing rafts and the potential impact of changing membrane composition or environmental variables. One of the central results from studies of laterally heterogeneous model membranes is the observation of inhomogeneities on two length scales, ranging from micron-sized domains [23] to domains of diameter smaller than 10 nm [24]. SANS is a technique able to detect formation and enable characterization of domains on length scales intermediate between these sizes. In the example of Fig. 6 the pattern A comes from a contrast matched ULV (mixture of deuterated saturated and unsaturated lipids and cholesterol at 50 °C where lipid components are homogeneously mixed) while B is from ULVs containing segregated domains (lower temperature). For the curve A, the scattering from the vesicles is minimized and the signal comes from the difference in $\rho$ between the chains and the headgroups of the lipids. When the samples are cooled, ULV exhibiting lateral segregation will show an additional contribution to the scattered intensity due to the contrast

between domains (profile B). From the data analysis domains were detected of sizes ranging from 7 to 40 nm. This work also showed that neither vesicle size nor curvature greatly modify domain formation in these membranes.

### 4.2. Diffraction

Experiments are performed in reflection conditions, generally with a monochromatic beam and recording the intensity with $\theta$–$2\theta$ scans in a typical range of 5 to 50 degrees. The diffracted pattern presents a series of peaks that follows the Bragg's law.

Diffraction measurements are used for studying periodic systems and allow the determination of the scattering profile perpendicular to the plane of incidence. For the study of model membranes they will require multilamellar systems (of several hundreds bilayers) with a fairly good planar orientation (typically of less than a few degrees). It is a technique useful for answering specific questions as the location of an object within the lipid bilayer (for example cholesterol or peptides).

Diffracted reflections give the following information: (i) the number of diffracted peaks (typically from 5 to 10 orders) gives indications on the order of the sample; (ii) the angular position of the peaks corresponds to the periodicity (typically of about 50–100 Å); (iii) for each order the integrated intensity of the peak is proportional to the square root of the structure factor modulus.

The searched information, i.e., the scattering profile in real space (normal to the surface), is derived from the Fourier transform of the structure factors (the summation is done over all measured orders). The absolute resolution is generally low and depends on the number of diffracted peaks ($\sim$5 Å if only 5 orders are measured). For a typical membrane it will be possible to distinguish between the water region, the head groups and the tails groups (the $CH_2$ and $CH_3$ groups). The combination of $H_2O/D_2O$ exchange, as well as specific labeling, allow the determination of the mean label position up to an accuracy of the order or better than 1 Å, for samples in the gel phase [25]. For more details on this technique, see [26–28] and references therein.

The use of aligned lipid/water systems has allowed one to gain new insights into the structure of a variety of lipid phases. Compared to liposomes, these *stacked* bilayers in saturated water atmosphere may show a reduced level of hydration and therefore of repeat spacing (*vapour pressure paradox* [29]). Studies of the effect of hydration are important to understand fusion mechanisms. Recent work [30] describes neutron diffraction measurements on a mixture of headgroup deuterated DOPC-d13 and non-deuterated DOPE to study the lipid distribution in the distorted hexagonal phase. The 1:1 lipid mixture in full hydration and 25 °C was in a homogeneous lamellar phase. Upon dehydration the mixture transformed to a rhombohedral phase, then to a distorted inverted hexagonal phase, and finally to a regular inverted hexagonal phase. An example of the pattern found on a two-dimensional detector is given in Fig. 7. Diffraction intensities measured while varying the $D_2O/H_2O$ ratio in the humidity were used to solve the phase problem. For the first time it was shown that when a monolayer of a homogeneous lipid mixture is bent, the lipid components are partially demixed in reaching the free energy minimum. The conclusion of the study and its biological relevance is that demixing of lipid components is a potential variable in the free energy of bending transitions and also that, in the search for the mechanisms by which proteins induce bending transitions of lipid bilayers, it is important to study both the dehydration-induced and temperature-induced lipid phase transitions.

### 4.3. Reflectivity

While SANS and neutron diffraction measurements have been used for decades for the structural characterisation of lipid bilayers, the use of neutron reflectivity in this field is much more recent. Specular reflectivity allows the determination of the structure and composition of matter perpendicular to a surface or an interface, typically with length scales from 10 Å to 5000 Å. Experiments are performed in reflection at grazing incidence ($\theta_i$ varies typically from 0.01 to 5 degrees). The sample and the detector move in order to keep the angle of incidence equal to the angle of reflection. Samples must be planar, homogeneous and smooth.

When a beam arrives on a planar surface, at a grazing angle, the atoms of the surface act as a mirror and, as for light, the beam is nearly totally reflected. When a thin layer is deposited on such surface, there will be interference between the beam reflected by the surface and the beam reflected by the interface according to the equation:

$$R(q) = \frac{16\pi^2}{q^2}\left|\hat{\rho}(q)\right|^2 \tag{3}$$

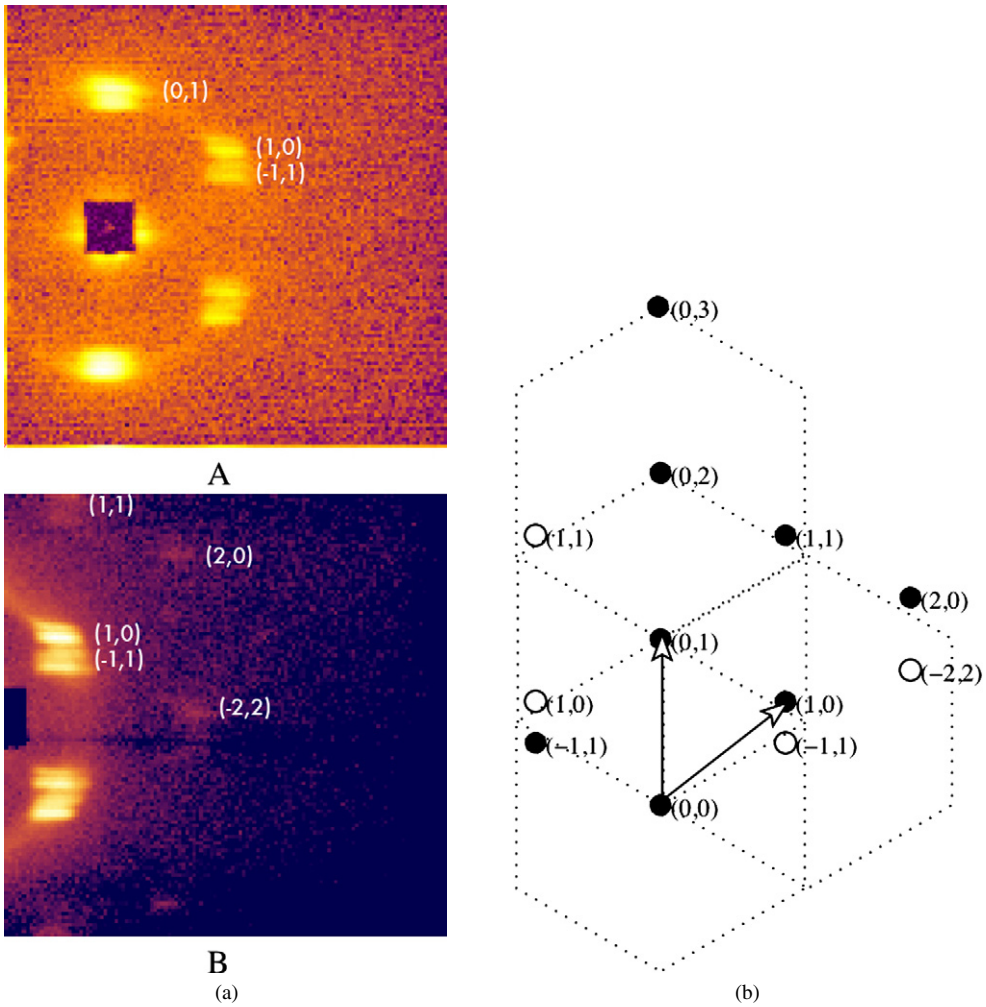


Fig. 7. (a) Reflection image produced by a mixture of headgroup deuterated DOPC-d13 and non-deuterated on the area detector of the D16 diffractometer at the ILL. The sample substrates were held approximately horizontal. (A) The detector was 4.98° from the incident beam and the exposure time was 5 min. The peaks were smeared in the vertical direction due to the vertical beam divergence. (B) The detector was at 12° from the incident beam, and the exposure time was 7 h to detect possible higher orders in the high $qx$ region. The peaks are identified by referring to the (b) distorted hexagonal (2D monoclinic) lattice. $(0, 1)$, $(1, 0)$, and $(-1, 1)$ are visible in (A). $(1, 1)$, $(1, 0)$, $(-1, 1)$, $(2, 0)$, and $(-2, 2)$ are visible in (B). The weak peak near the geometrical center of the detector in (B) belongs to the coexisting hexagonal phase.

where $R(q)$ is the reflected over the incoming intensity as a function of $q$ and $\hat{\rho}(q)$ is the one-dimensional Fourier transform of $\rho(z)$, that is:

$$\hat{\rho}(q) = \int_{-\infty}^{+\infty} \exp(-\mathrm{i}qz)\rho(z)\,\mathrm{d}z \tag{4}$$

$\rho(z)$, the scattering length density, being a function of the distance perpendicular to the interface. The approximate relations above are given to indicate the direct relation between reflectivity and structure, but using the optical matrix method [31], it is possible to calculate reflectivity exactly for any given model of the interface.

High resolution can be obtained for aqueous systems when it is possible to measure the reflectivity profiles of the same sample with different $H_2O/D_2O$ content [32,33]. While specular reflection gives information in the direction perpendicular to the interface, the lateral structure of the interface may be probed by the non-specular scattering measured at reflection angles different from the specular one [34].

Reflectivity techniques are well suited for studies of monolayers at air/liquid interfaces. A review of structural models of lipid surface monolayers from X-ray and neutron reflectivity measurements is found in [35].

Phospholipid bilayers adsorbed on surfaces and in contact with an aqueous environment are biologically more relevant model membranes than monolayers (Fig. 3(b)). For these systems, neutrons provide a great advantage with respect to X-rays, since X-rays are adsorbed both by the solid substrate and by the aqueous solution; nevertheless studies at the solid/liquid interface, mainly performed at synchrotron sources, have started to appear in the literature [10, 36,37]. The advantage with respect to SAS or diffraction studies on multilamellar systems is that the information is not averaged over a high number of bilayers.

Krueger et al. [38] have been able to obtain reflectivities down to $10^{-8}$ and $q$ out to 0.7 $\text{Å}^{-1}$ by decreasing the thickness of the water in contact with a hybrid bilayer (formed by an alkanethiol chemisorbed to a gold surface and a phospholipid layer) down to 15 μm. In these conditions, the resolution of the neutron reflectivity experiments is limited only by the roughness of the supporting substrate. The position of a membrane active peptide (melittin) in the system was determined.

A recent interesting example is the study of the effect of the phospholipase enzyme A2 catalyzed hydrolysis of supported phospholipid bilayers using neutron reflection and ellipsometry. At the hydrophilic silica-water interface, hydrolysis of phosphatidylcholine bilayers by phospholipase A2 from *Naja mossambica mossambica* venom is accompanied by destruction of the bilayer. Neutron reflectivity measurements indicated that the enzyme penetrates into the bilayers in increasing order for DOPC, POPC, and DPPC, while the amount of enzyme adsorbed at the interface is smallest for DPPC and exhibits a maximum for POPC [39]. Here deuterium labeling was cleverly used to study the fate of the reaction products. In fact, hydrolysis of a single-chain deuterium labeled d31-POPC revealed that there is a significant asymmetry in the distribution of the reaction products between the membrane and the aqueous environment. The lyso-lipid is unambiguously found to leave the membrane, while the amount of fatty acid increases. The number of PLA2 enzymes bound to the membrane increases with increasing fatty acid content, confirming that the reaction is autocatalytic, but also that lipid substrate undergoes dramatic compositional changes during the hydrolytic reaction. These results constitute the first direct measurement of the membrane structure and composition together with the location and amount of the enzyme during hydrolysis, which are discussed in terms of a model of fatty-acid mediated activation of PLA2, as sketched in Fig. 8.

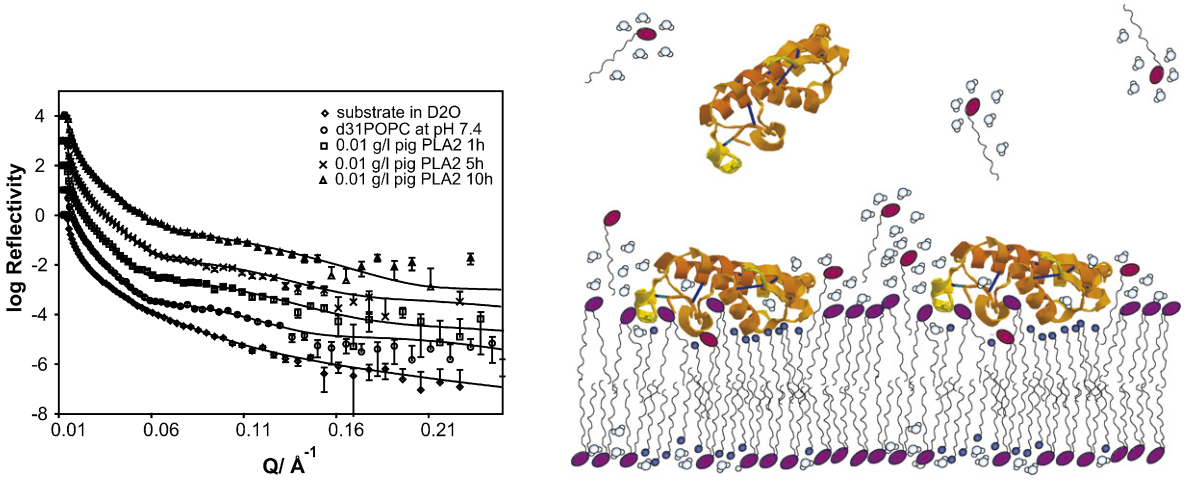


(a) (b)

Fig. 8. (a) Specular reflectivity of a supported d31-POPC bilayer at the Silica–$D_2O$ interface recorded before and during porcine pancreatic PLA2 hydrolysis. (Open diamonds) substrate reflectivity in $D_2O$, (Open circles) d31-POPC bilayer at in 10 mM Tris-$D_2O$ pH 7.4, (open squares) d31-POPC bilayer 1 h after injection of 0.01 mg $\text{ml}^{-1}$ PLA2, (crosses) d31-POPC bilayer 5 h after PLA2 injection and (open triangles) d31-POPC bilayer 10 h after PLA2 injection. Curves are shifted for clarity. From the shape of the reflectivity profiles it can be seen that as the reaction proceeds data from the bilayer loose the characteristic fringe at $q \sim 0.06$ $\text{Å}^{-1}$ and look much more like data from the bare surface. For more details see [39]. Data collected on D17 at the Institut Laue-Langevin. (b) Schematic model of a possible PLA2 interaction with a phospholipid bilayer based on the box models used to fit neutron reflectivity data as presented [39]. The enzyme resides at the lipid–water interface and partially penetrates into the bilayer. Fatty acid (small head group) accumulates in the bilayer as the lyso-phospholipid (large head group) partitions into the solution.

## 5. Results from dynamics studies

Dynamical properties are often less well understood in biomolecular systems, but are important for many fundamental biomaterial properties as, e.g., elasticity properties and interaction forces. Furthermore, lipid membrane dynamics on small molecular length scales determines, or strongly affects, functional aspects, like diffusion and parallel or perpendicular transport through a bilayer. The specific advantages of neutron scattering to study fluctuations of phospholipid membranes on lateral length scales between μm down to a few Å can give unique insights.

The spectrum of fluctuations in biomimetic and biological membranes covers a large range of time and length scales ranging from the long wavelength undulation and bending modes of the bilayer with typical relaxation times of nanoseconds and lateral length scales of several hundred lipid molecules, down to the short-wavelength, picosecond density fluctuations involving neighboring lipid molecules. New developments and improvements in neutron scattering instruments, sample preparation and environment and, eventually, more and more powerful neutron sources open up the possibility to study collective excitations, i.e. phonons, in artificial and biological membranes. The combination of various inelastic neutron scattering techniques enlarges the window of accessible momentum and energy transfers—or better, accessible length and time scales—and allows one to study structure and dynamics on length scales ranging from the nearest-neighbor distances of lipid molecules to length scales of more than 100 nm, covering time scales from about 0.1 ps to almost 1 μs. The fluctuations are quantified by measuring the corresponding dispersion relations, i.e. the wave vector-dependence of the excitation frequencies or relaxation rates. Because biological materials lack an overall crystal structure, in order to fully characterize the fluctuations and to compare experimental results with membrane theories, the measurement must cover a very large range of length and time scales. By using multiple instruments, from spin-echo to triple-axis spectrometers, these fluctuations have successfully been probed over the desired range of length and time scales [41–45]. Fig. 9(a) sketches some of the collective motions that can be accessed.

Only recently, the first inelastic scattering experiments in phospholipid bilayers to determine collective motions of the lipid acyl chains and in particular the short wavelength dispersion relation have been performed using inelastic X-ray [40] and neutron [41] scattering techniques. Note that only scattering experiments give wave vector resolved ac-

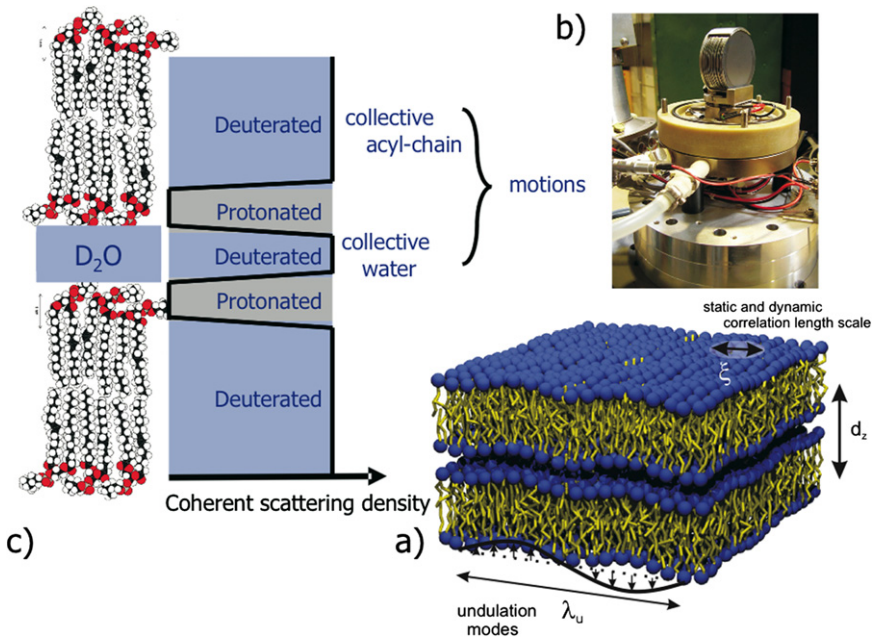


Fig. 9. (a) Collective excitations are coherent motions of several membrane molecules, as, e.g., the long wavelength bending modes of the membranes with wavelength $\lambda_u$. (b) Photograph of the sandwich sample mounted in the humidity chamber to control temperature and hydration during the experiment. (c) Sketch of a double bilayer of chain deuterated DMPC, hydrated with $D_2O$, together with the corresponding coherent scattering density. This type of sample preparation makes the neutron experiment basically sensitive to collective motions of lipid acyl chains and hydration water.

cess to dynamical properties, which are important for associating relaxation times with specific molecular components and motions. While in protonated samples the incoherent scattering is normally dominant and the time-autocorrelation function of individual scatterers is accessible in neutron scattering experiments, (partial) deuteration emphasizes the coherent scattering and gives access to collective motions by probing the pair correlation function. In the case of single membranes the inelastic neutron scattering signal is by far not sufficient for a quantitative study of the inelastic scattering. Highly oriented multilamellar membrane stacks of several thousands of lipid bilayers were therefore prepared by spreading lipid solution of typically 25 mg/ml lipid in trifluoroethylene/chloroform (1:1) on 2″ silicon wafers. Twenty such wafers separated by small air gaps were combined and aligned with respect to each other to create a 'sandwich sample' (as shown in Fig. 9(b)) consisting of several thousands of highly oriented lipid bilayers (total mosaicity about 0.5°), with a total mass of about 400 mg of deuterated DMPC. The mosaicity of the sandwich is composed of the alignment of the bilayers within the stack on one wafer and of the orientation of different wafers with respect to each other. The use of well oriented samples leads to well localized elastic and inelastic signals in reciprocal space and allows one to distinguish motions in the plane of the membranes ($q_\parallel$) and perpendicular to the bilayers ($q_z$). During the experiments, the membranes were kept in a 'Humidity Chamber' to control temperature and humidity and hydrated with $D_2O$ from the vapor phase, as also shown in Fig. 9(b). For the following experiments, the collective motions of the lipid acyl chains have been emphasized over other contributions to the inelastic scattering signal by using partially deuterated lipids, as pictured in Fig. 9(c). The measurement of these motions provides not only a deeper understanding of membrane micromechanical properties down to the molecular scale, but also sheds some light on the processes which are essential for the formation of contacts between cells and between cells and solid surfaces.

### *5.1. Dispersion relations*

Fig. 10(a) shows the dispersion relations measured by neutron three-axis, backscattering and spin-echo spectroscopies. Data have been taken in the fluid phase of deuterated DMPC stacked bilayers. The respective type of excitation, i.e., propagating, relaxation or oscillating modes, thereby depends on length and time scales. Propagating or oscillating modes have well defined eigenfrequencies and lead to inelastic excitations at energy values $\hbar\omega <> 0$. Relaxations give rise to a quasielastic broadening $\Delta\omega$, centered at $\hbar\omega = 0$. The dotted vertical lines emphasize two prominent $q_\parallel$ values, i.e., intrinsic lateral length scales, of the model membranes. $q_0 \approx 1.4$ Å$^{-1}$ corresponds to the nearest neighbour distance of the phospholipid acyl chains ($2\pi/q_0$); $q_0 \approx 0.015$ Å$^{-1}$ marks the transition from the film to the bulk elasticity regime, as we will discuss below. At both $q_\parallel$ values, the corresponding dispersion relations show distinct anomalies as kinks or minima.

#### *5.1.1. Triple-axis spectrometry*

Fast motions in the ps time range due to sound propagation in the plane of the bilayer are best measured on triple-axis spectrometers. The energy of the incident and scattered neutrons are determined by Bragg scattering from crystal monochromators (graphite in most cases). Advantages of triple-axis spectrometers are their relatively simple design and operation and the efficient use of the incoming neutron flux for the examination of particular points in $(q, \omega)$ space. By varying the three axes of the instrument, the axes of rotation of the monochromator, the sample and the analyzer, the wave vectors $k_i$ and $k_f$ and the energies $E_i$ and $E_f$ of the incident and the scattered neutrons, respectively, can be determined. The momentum transfer to the sample, and the energy transfer, $\hbar\omega$, are then defined by the laws of momentum and energy conservation to $q = k_f - k_i$ and $\hbar\omega = E_i - E_f$. The accessible $(q, \omega)$ range is just limited by the range of incident neutron energies offered by the neutron guide as well as by mechanical restrictions of the spectrometer. Fig. 10(b) shows an energy scan at a $q_\parallel$-value of $q_\parallel = 1$ Å$^{-1}$, as an example. The excitation appears as small peak at about 6 meV which corresponds to an excitation period of about 0.7 ps or 1.4 THz. The particular shape of the corresponding dispersion relation (in Fig. 11) can qualitatively be explained. The basic scenario is the following: at small $q_\parallel$, longitudinal sound waves in the plane of the bilayer are probed and give rise to a linear increase of $\omega \sim q_\parallel$, saturating at some maximum value, before a pronounced minimum is observed at $q_0 \approx 1.4$ Å$^{-1}$, the first maximum in the static structure factor $S(q_\parallel)$ (the inter acyl chain correlation peak). $q_0$ can be interpreted as the quasi-Brillouin zone of a two-dimensional liquid. Collective modes with a wavelength of the average nearest neighbour distance $2\pi/q_0$ are energetically favorable. The static and dynamic disorder in the lipid bilayers finally leads to a

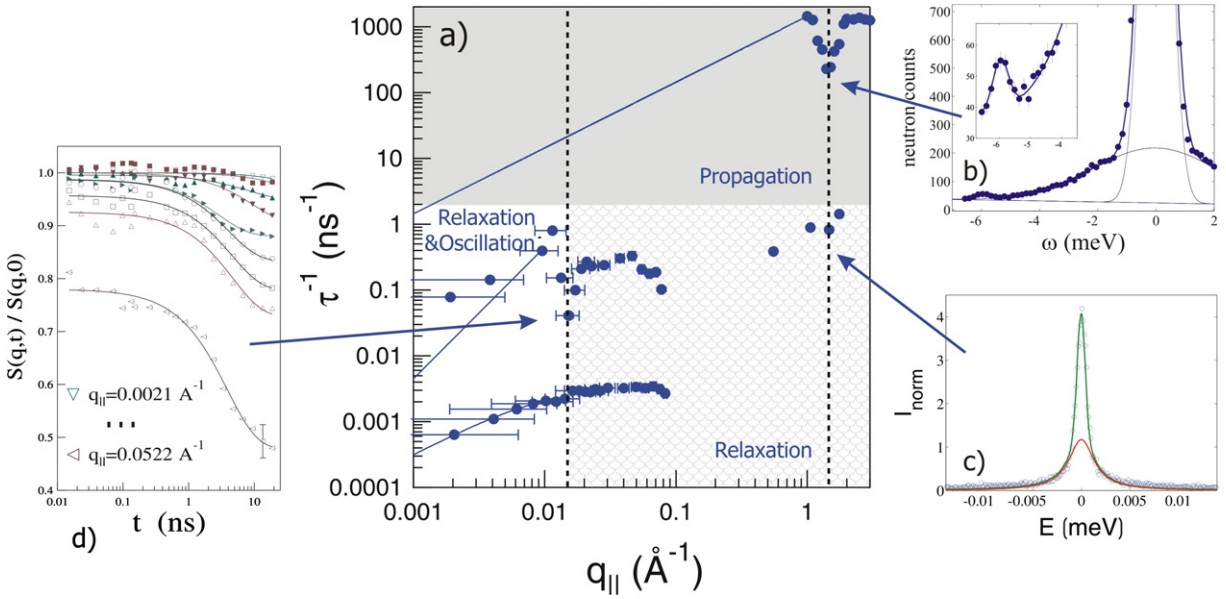


Fig. 10. (a) 'Neutron Window' of collective excitations in DMPC-d54 in the fluid phase. The measurements cover a lateral $q_\parallel$-range of $0.002\ \text{Å}^{-1} < q_\parallel < 3\ \text{Å}^{-1}$ and $1\ \mu\text{s} < \tau < 0.5$ ps. Regions assigned to propagating, relaxating, overdamped and oscillating modes are marked in the figure. (b) The domain of three-axes spectrometry is the detection of fast propagating picosecond motions at larger $q_\parallel$ values. The inset exemplary shows an excitation of the DMPC bilayer at $q_\parallel = 1\ \text{Å}^{-1}$. Solid lines are fits of theoretical models, as explained in [20] (data from IN12 and IN8 at the ILL). (c) Backscattering spectrometers are used to measure relaxations in the nanosecond time range at larger $q_\parallel$ values (data shown are from IN16 at the ILL). The inset shows quasielastic scattering integrated over $0.4\ \text{Å}^{-1} < q_\parallel < 0.65\ \text{Å}^{-1}$. Although the $q$ resolution of the spectrometer is much higher, five detector tubes have been summed up here to increase the statistics of the scattering signal. The darker line is a Lorentzian line shape. It has been convoluted with the resolution function to fit the data. (d) The range at small $q_\parallel$ and long relaxation times $\tau$ is accessible on spin-echo spectrometers (IN11 and IN15 at the ILL). Two relaxation processes are found on different time scales and both dispersion relations are shown in (a). The inset shows selected relaxation curves of the fast ($\tau \sim 10$ ns) process (the upper dispersion curve in (a)) for $q_\parallel$-values between 0.002 and 0.05 $\text{Å}^{-1}$. Solid lines are fits assuming single exponential decays.

minimum at finite energy values (soft-mode). A quantitative theory which predicts the absolute energy values of maximum and minimum on the basis of molecular parameters is absent so far. However, the dispersion relation can be extracted from molecular dynamics simulations by temporal and spatial Fourier transformation of the molecular real space coordinates [46] which shows excellent agreement with the data. Note that the dispersion relation found is similar to those in ideal liquids, as e.g. liquid argon [47,48], liquid neon [49] or liquid helium [50]. It seems that the interior of the lipid bilayer, the C-atoms or C–D groups of the lipid acyl chains, behave as a quasi liquid. In contrast to real liquids, the chain atoms of the lipid molecules are chemically bound to each other, leading to smaller mobility and diffusion and, as a consequence, pronounced excitations.

### *5.1.2. Spin-echo*

Fluctuations on the mesoscopic scale are determined by the elasticity parameters of the bilayers, i.e., the compressibility of the stacked membranes, B, and the bending modulus. The relaxations in this regime are in the nanosecond time-range with accompanying small $q$-values. Spin-echo spectrometers turned out to be highly suited for these experiments.

The spin-echo technique offers extremely high energy resolution from Larmor tagging the neutrons. A neutron spin-echo measurement is in essence a measurement of neutron polarization [51]. A polarized neutron beam passes through a magnetic field perpendicular to the neutron polarization. The neutron spin precesses before arriving at the sample, acquiring a precession angle $\phi_1$. At the sample, the beam is scattered before passing through a second arm, acquiring an additional precession angle $\phi_2$ in the reversed sense. For elastic scattering, the total precession angle is $\Delta\phi = \phi_1 - \phi_2 = 0$ for all incoming neutron velocities.

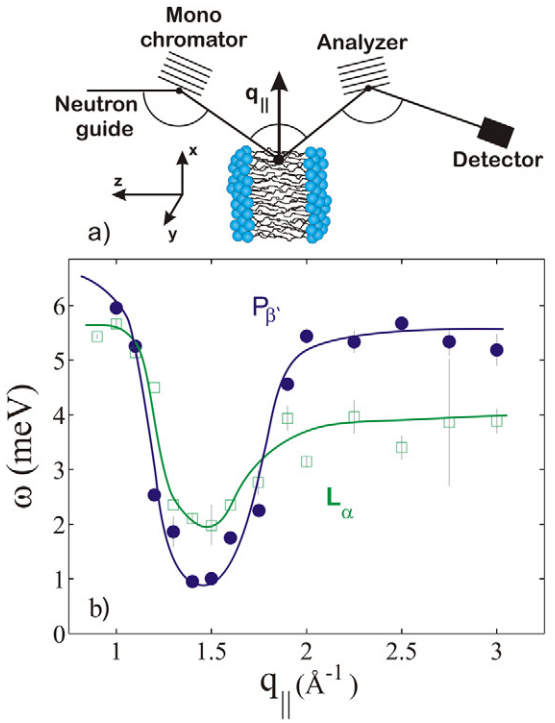


Fig. 11. (a) Schematic of a triple-axis spectrometer. (b) Short wavelength dispersion relations in the gel (P$\beta'$) and fluid phase L$\alpha$ of the DMPC bilayers.

If the neutron scatters inelastically by a small energy transfer $\hbar\omega$, there will be a linear change $\Delta\phi = \tau\omega$ with $\tau$ being a real time in the case of quasielastic scattering. The spin-echo technique thus works in the time domain and measures the intermediate scattering function $S(q_\parallel, t)$ in contrast to the three-axis and backscattering technique. For a quasielastic response, assumed to have Lorentzian lineshape with half-width $\Gamma$, the polarization will then show a single exponential decay PNSE $= P_s \mathrm{e}^{-\Gamma t}$. Fig. 10(d) shows the intermediate scattering function $S(q_\parallel, t)$ for selected $q_\parallel$ values for spin-echo times 0.001 ns $< t <$ 20 ns, which exhibits distinct single-exponential relaxation steps. According to linear smectic elasticity theory, thermal fluctuations in the fluid phase of the membranes in the mesoscopic regime probed by spin-echo are governed by the free energy functional (Hamiltonian):

$$H = \int_A \mathrm{d}^2 r \sum_{n-1}^{N-1} \left( \frac{1}{2} \frac{B}{d} (u_{n+1} - u_n)^2 + \frac{1}{2} \kappa \left( \nabla_\parallel^2 u_n \right)^2 \right) \tag{5}$$

where $\kappa$ denotes the bilayer bending rigidity, $A$ the area in the $xy$-plane, $N$ the number of bilayers, and $u_n$ the deviation from the average position $n \cdot d$ of the $n$th bilayer, $d$ is the lamellar spacing. $B$ and $K = \kappa/d$ are elastic coefficients, governing the compressional and bending modes of the smectic phase, respectively. Note that the surface tension $\sigma$ can usually be neglected because of the boundary conditions, i.e., infinitely large membranes the rims of which are not clamped and small amplitudes of the fluctuations. Fig. 12 shows the corresponding dispersion relation in DMPC for different temperatures in the gel ($T = 19\,^\circ$C), the fluid (30 °C) phase and at an intermediate temperature, just above the main transition in phospholipid bilayers. Again, we can give qualitative arguments to explain the shape of the upper dispersion relation with relaxation rates between 1 and 10 ns: for $q_\parallel$ values smaller than $q_0 \approx 0.015$ Å$^{-1}$ (on length scales of several hundred lipid molecules), the lipid bilayers behave as liquid films and the corresponding dispersion relation shows a $q_\parallel^2$ dependence, basically determined by the viscosity of the water layer in between the stacked membranes [52,53]. Note that this regime does not contain microscopic information about the bilayers ('macroscopic regime' or 'film regime'). With increasing $q_\parallel$, a bifurcation occurs at $q_0$ where we start to probe the bulk elasticity parameters $B$ (compressibility) and $K$ (bending modulus) of the bilayers ('bulk elasticity regime'). Because energy is now dissipated in the elastic degrees of freedom, the character of the motion changes

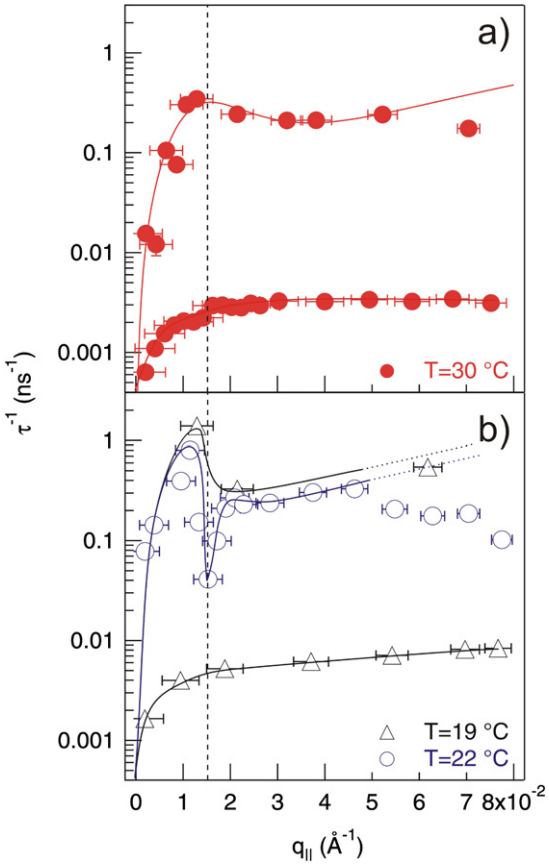


Fig. 12. (a) Mesoscopic dispersion relation in the fluid phase at $T = 30\,^{\circ}\mathrm{C}$. The solid line is a fit to a smectic hydrodynamic theory. (b) Dispersion relations of DMPC in the gel (19 °C) and in the fluid phase (22 °C), in the range of critical swelling. A pronounced soft mode is observed at $q_0 = 0.015\ \mathrm{\AA}^{-1}$ at 22 °C (dotted vertical line). Solid lines in (b) are guides to the eye.

from propagating or oscillating to purely over damped relaxation. $B$ and $K$ can be determined from fits of theoretical models to the data. The experimental data in the fluid phase can be fitted to a smectic hydrodynamic theory and the elasticity parameters $B$ and the viscosity $\eta$ determined to $B = 1.08 \times 10^7\ \mathrm{J\,m^{-3}}$, $= 14.8\ \mathrm{k_B\,T}$ and $\eta = 0.016\ \mathrm{Pa\,s}$. The viscosity of the membrane water appears to be much higher as compared to bulk water (0.001 Pa s) pointing to distinctly different dynamical properties of the two-dimensional layer of hydration water. As a remarkable feature we find a soft-mode, i.e. an extreme softening of the bilayers, in the critical swelling regime at $T = 22\,^{\circ}\mathrm{C}$, which occurs on a well-defined length-scale of about 45 nm, probably related to the formation of gel and fluid domains in the co-existence region. While the upper dispersion branch is well described by present theories, the slow dispersion branch with relaxation rates of about 100 ns (the lower dispersion curve in Fig. 12(a)) may be attributed to an additional surface relaxation mode.

### *5.1.3. Backscattering*

These experiments can be complemented by μeV energy resolved spectra, achieved by the neutron backscattering technique. In backscattering experiments the scattering function $S(Q, \omega)$ is directly measured analogously to three-axis spectroscopy, but contrarily to neutron spin-echo. The high resolution obtained

$$\frac{\Delta\lambda}{\lambda} = \frac{\Delta d}{d} + \frac{\Delta\theta}{\tan\theta} \tag{6}$$

in exact backscattering is easily shown by computing the first derivative of Bragg's law (Eq. (1)), where $\lambda$ is the neutron wavelength, $d$ the monochromator crystal lattice spacing and $\theta$ the angle of incidence of the neutron beam with respect to the crystal surface. From this equation it becomes clear that the monochromaticity is maximized when the angle

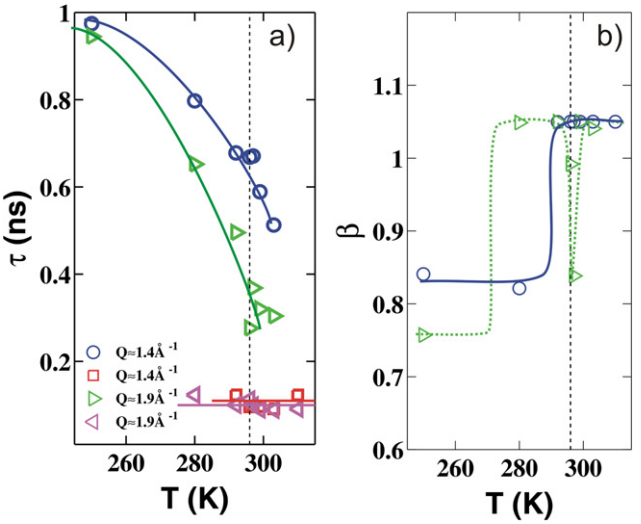


Fig. 13. (a) Relaxation times of the lipid acyl chain and the membrane hydration water as determined from fits to quasi elastic data. (b) Exponents of the exponential decay as determined from fits of the intermediate scattering function. Solid lines are guides to the eye.

of incidence is 90° with respect to the monochromator and analyzer crystal surface of a spectrometer. Overdamped modes appear as quasielastic broadening, as shown in Fig. 10(c). In combination with the three-axis technique, where propagating modes in the picosecond range are probed, the backscattering technique thus gives access to relaxations on the same length scale, but in the nanosecond time range. By careful analysis of the 'elastic' scattering, that is scattering which is elastic within the excellent energy resolution of 1 μeV, scattering contributions of the lipids, in particular the lipid acyl chains, and the membrane water, i.e. molecules in the water layer in between the stacked membranes, could be identified by their respective $q_{\|}$-values. The hydration water turns out to have a freezing temperature of 271 K, 7 K below the freezing of bulk heavy water ($D_2O$). A recent experiment allowed one to determine the relaxation rates of acyl chains and water molecules separately, but simultaneously. From a combined analysis in the energy and time domains, the stretching exponent, $\beta$, for the two processes, i.e. the deviation from single exponential decays of the corresponding correlation functions could also be determined. The relaxation dynamics thus highly depends on the local environment in the regimes where lipid tails and water molecules are 'frozen' ($T < 294$ K for the lipids and $T < 271$ K for the water) with values for $\beta$ of $\beta < 1$. In the respective fluid phases, the relaxations turn into single exponentials. Fig. 13 shows the time-dependence of the corresponding relaxation times (a) together with the stretching parameter $\beta$ (b). Note that in the regime of critical swelling, the water dynamics again develops a distinct 'stretched' character. Elaborate future experiments should allow one to simultaneously determine complete dispersion relations of lipids and water to quantify the corresponding dynamics. It is now widely accepted that the dynamics of biological systems cannot be fully understood without understanding the dynamics of the aqueous surrounding as well, so that these experiments provide a unique and important insight.

## 6. Future challenges

Lipid bilayers are probably the most natural substrate on which to test lipid–peptide or lipid–protein interactions. Scattering techniques are an important tool for the study of these interactions. So far most of the experimental effort has concentrated on the study of lipid bilayers alone and on the research of suitable models for membranes. These studies have advanced to a point that more and more complex systems are being considered, including the use of small peptides, membrane proteins, fusion proteins, enzymes and drug delivery systems.

A review on recent developments of neutron reflectivity methods for the study of peptide and protein interactions with model membranes can be found in [54].

Perspectives of grazing incidence surface scattering in biophysics are the possibility of detecting how adsorbed peptides or proteins correlate with the bilayer fluctuations in position, density, thickness, and possibly lipid composition. Joint X-ray (for resolution) and neutron (for composition) investigations could be sensitive to the protein itself:

overall shape, orientation and position. For peptides, which are more difficult to detect, the position and orientation can, in principle, be determined as well.

The deuteration of proteins is becoming an active field of research. The use of fully deuterated or partially deuterated proteins will open up new possibilities in the study of lipid protein interactions or protein structures at lipid surfaces (during, for example, events of fusion or cellular recognition).

Foreseen improvement of neutron techniques for off-specular measurements, for in-plane structural determinations and for the study of liquid–liquid interfaces, will certainly lead to new science being done in the field of model membranes.

Because of optimized setups and sample preparation, neutron scattering experiments supply for the first time sufficiently strong (coherent) inelastic signals for quantitative analysis. The measurements offer a large window of length and time scales, ranging from about 0.1 ps to almost 1 μs and length scales from 3 Å to about 0.1 μ m to test and refine theoretical models of dynamics in biomimetic and biological membranes. Comparison with present membrane theories gives a qualitative agreement of experiment and theory, only. The reason for that certainly lies in the fact that so far only information from elastic scattering was available to test theoretical predictions. Intensity is clearly the limiting factor for dynamical studies. The next generation of neutron scattering instruments and neutron sources will allow one to investigate protein dynamics of proteins embedded in membranes, i.e., in their natural environment. The protein dynamical scattering can be well identified and separated by its location in reciprocal space.

## References

[1] O. Mouritsen, O. Andersen, In search of a new biomembrane model, Biologiske, 1998.
[2] R. Lipowsky, E. Sackmann (Eds.), Structure and Dynamics of Membranes, Handbook of Biological Physics, vol. 1, Elsevier, Amsterdam, 1995.
[3] L. Rilfors, G. Lindblom, Colloids and Surfaces B: Biointerfaces 26 (2002) 112–124.
[4] G.L. Gaines, Insoluble Monolayers at Liquid–Gas Interface, Interscience Publishers, New York, 1966.
[5] E. Sackmann, Science 271 (1996) 43–48.
[6] T.H. Watts, A.A. Brian, J.W. Kappler, P. Marrack, H.M. McConnell, Proc. Nat. Acad. Sci. USA 81 (1984) 7564.
[7] L. Tamm, H. McConnell, Biophys. J. 47 (1985) 105–113.
[8] M. Tanaka, E. Sackmann, Nature 437 (2005) 656–663.
[9] T. Charitat, E. Bellet-Amalric, G. Fragneto, F. Graner, Eur. Phys. J. B 8 (1999) 583–593.
[10] J. Daillant, E. Bellet-Amalric, A. Braslau, T. Charitat, G. Fragneto, F. Graner, S. Mora, F. Rieutord, B. Stidder, Proc. Nat. Acad. Sci. 102 (33) (2005) 11639–11644.
[11] G. Fragneto, T. Charitat, E. Bellet-Amalric, R. Cubitt, F. Graner, Langmuir 19 (2003) 7695–7702.
[12] B. Stidder, G. Fragneto, S.J. Roser, Langmuir 21 (20) (2005) 9187–9193.
[13] B. Stidder, G. Fragneto, R. Cubitt, A.V. Hughes, S. Roser, Langmuir 21 (19) (2005) 8703–8710.
[14] S. Lecuyer, G. Fragneto, T. Charitat, Eur. Phys. J. E 21 (2006) 153–159.
[15] A. Tardieu, V. Luzzati, F.C. Reman, J. Mol. Biol. 75 (1973) 711–733.
[16] J. Katsaras, Biophys. J. 75 (5) (1998) 2157–2162.
[17] M. Vogel, C. Munster, W. Fenzl, T. Salditt, Phys. Rev. Lett. 84 (2) (2000) 390–393.
[18] J. Pencer, T. Mills, V.N.P. Anghel, S. Krueger, R.M. Epand, J. Katsaras, Eur. Phys. J. E 18 (2005) 447–458.
[19] S.M. Fahsel, E.M. Pospiech, M. Zein, T.L. Hazlet, E. Gratton, R. Winter, Biophys. J. 83 (2002) 334–344.
[20] J. Katsaras, T. Gutberlet (Eds.), Lipid Bilayers: Structure Interactions, Springer, 2000.
[21] D. Uhíková, N. Kucerka, A. Islamov, V. Gordeliy, P. Balgavy, Gen. Physiol. Biophys. 20 (2001) 183–189.
[22] N. Kucerka, M.-P. Nieh, J. Pencer, T. Harroun, J. Katsaras, Curr. Opin. Colloid Interface Sci. (2007), 10.1016/j.cocis.2006.11.006.
[23] S.L. Veatch, S.L. Keller, Biophys. J. 85 (2003) 3074.
[24] J.R. Silvius, Biophys. J. 85 (2003) 1034.
[25] V.I. Gordeliy, N.I. Chernov, Acta Cryst. D 53 (1997) 377–384.
[26] G. Buldt, H.U. Gally, A. Seelig, J. Seelig, G. Zaccai, Nature 271 (1978) 182–183.
[27] G. Buldt, J. Seelig, Biochem. 19 (1980) 6170–6175.
[28] G. Büldt, H.U. Gally, J. Seelig, G. Zaccai, Mol. Biol. 134 (1979) 673–691.
[29] R.P. Rand, V.A. Parsegian, Biochim. Biophys. Acta 998 (1989) 351–376.
[30] L. Ding, T.M. Weiss, G. Fragneto, W. Liu, L. Yang, H.W. Huang, Langmuir 21 (2005) 203–210.
[31] O.S. Heavens, Optical Properties of Thin Films, Butterworth, London, 1955.
[32] G. Fragneto, T. Charitat, P. Dubos, F. Graner, E. Bellet-Amalric, Langmuir 2 16 (2000) 4581–4588.
[33] J. Penfold, R.K. Thomas, J. Phys. Condens. Matter 2 (1990) 1369–1412.
[34] R. Pynn, Phys. Rev. B 45 (2) (1992) 602–612.
[35] M. Schalke, M. Losche, Adv. Colloid Interface Sci. 88 (2000) 243–274.
[36] C.E. Miller, J. Majewski, T.L. Kuhl, Colloids Surfaces A (2006) 434–439.

[37] E. Nováková, K. Griewekemeyer, T. Salditt, Phys. Rev. E 74 (2006) 051911 (9 pages).
[38] S. Krueger, C.W. Meuse, C.F. Majkrzak, et al., Langmuir 17 (2000) 511–521.
[39] H.P. Wacklin, F. Tiberg, G. Fragneto, R.K. Thomas, BBA—Biomembranes 1768 (2007) 1036–1049.
[40] S. Chen, C. Liao, H. Huang, T. Weiss, M. Bellissent-Funel, F. Sette, Phys. Rev. Lett. 86 (2001) 740–743.
[41] M.C. Rheinstädter, C. Ollinger, G. Fragneto, F. Demmel, T. Salditt, Phys. Rev. Lett. 93 (2004) 108107 (4 pages).
[42] M.C. Rheinstädter, T. Seydel, F. Demmel, T. Salditt, Phys. Rev. E 71 (2005) 061908 (8 pages).
[43] M.C. Rheinstädter, W. Häußler, T. Salditt, Phys. Rev. Lett. 97 (2006) 048103 (4 pages).
[44] M.C. Rheinstädter, T. Seydel, T. Salditt, Phys. Rev. E 75 (2007) 011907 (5 pages).
[45] M.C. Rheinstädter, T. Seydel, W. Häußler, T. Salditt, J. Vac. Soc. Technol. A 24 (2006) 1191–1196.
[46] M. Tarek, D. Tobias, S.-H. Chen, M. Klein, Phys. Rev. Lett. 87 (2001) 238101 (4 pages).
[47] I. de Schepper, P. Verkerk, A. van Well, L. de Graaf, Phys. Rev. Lett. 50 (1983) 974–977.
[48] A. van Well, P. Verkerk, L. de Graaf, J.-B. Suck, J. Copley, Phys. Rev. A 31 (1985) 3391–3414.
[49] A. van Well, L. de Graaf, Phys. Rev. A 32 (1985) 2396–2412.
[50] H. Glyde, Excitations in Liquid and Solid Helium, Oxford Series on Neutron Scattering in Condensed Matter, vol. 9, Clarendon Press, Oxford, 1994.
[51] F. Mezei (Ed.), Neutron Spin Echo, Springer, Berlin, 1980.
[52] V. Romanov, S. Ul'yanov, Phys. Rev. E 63 (2001) 031706 (11 pages).
[53] V. Romanov, S. Ul'yanov, Phys. Rev. E 66 (2002) 061701 (9 pages).
[54] S. Krueger, Curr. Opin. Colloid Interface Sci. 6 (2001) 111–117.